

# Delocalizing effect of the Hubbard repulsion for electrons on a two-dimensional disordered lattice

Bhargavi Srinivasan<sup>(a)</sup>, Giuliano Benenti<sup>(a,b)</sup>, and Dima L. Shepelyansky<sup>(a)</sup>

<sup>(a)</sup>Laboratoire de Physique Quantique, UMR 5626 du CNRS, Université Paul Sabatier, 31062 Toulouse Cedex 4, France

<sup>(b)</sup>Center for Nonlinear and Complex Systems, Università degli Studi dell'Insubria and

Istituto Nazionale per la Fisica della Materia, Unità di Como, Via Valleggio 11, 22100 Como, Italy

(January 31, 2003)

We study numerically the ground-state properties of the repulsive Hubbard model for spin-1/2 electrons on two-dimensional lattices with disordered on-site energies. The projector quantum Monte Carlo method is used to obtain very accurate values of the ground-state charge density distributions with  $N_p$  and  $N_p + 1$  particles. The difference in these charge densities allows us to study the localization properties of an added particle. The results obtained at quarter-filling on finite clusters show that the Hubbard repulsion has a strong delocalizing effect on the electrons in disordered 2D lattices. However, numerical restrictions do not allow us to reach a definite conclusion about the existence of a metal-insulator transition in the thermodynamic limit in two-dimensions.

PACS numbers: 71.10.Fd, 73.20.Fz, 71.23.An

## I. INTRODUCTION

The interplay between disorder and electron-electron interactions has been a subject of intense activity in the last few years. Recent experiments have shown the existence of an apparent metal-insulator transition (MIT) in two-dimensional (2D) semiconductor devices [1]. This observation came as a surprise to the community, since the scaling theory of localization, developed for disordered, non-interacting systems predicts insulating states even for infinitesimal disorder strengths [2]. Therefore, these experiments have promoted intense theoretical activity. There is at present no consensus and considerable controversy surrounds this problem [1]. A novel feature of the experimental high mobility samples investigated is their exceptionally low electronic density  $n_s$ . This leads to an unusually high value of the dimensionless parameter  $r_s \propto n_s^{-1/2}$  of up to 80. The parameter  $r_s$  sets the scale of electron-electron interaction  $E_{e-e}$  as compared to the Fermi energy  $E_F$  through  $r_s \approx E_{e-e}/E_F$ . Thus the question of electron-electron interaction effects becomes important in these disordered systems.

The analytical treatment of the problem of disordered, interacting electrons is possible only in some limiting cases. The effects of weak interactions in disordered systems have been studied in great detail in the metallic (delocalized) regime [3]. The other extreme, corresponding to the strongly localized system can be treated by mean-field methods [4]. Although these analytical approaches have provided many useful physical results, the general treatment of disordered quantum many-body systems remains an unsolved problem. Indeed, one of the most powerful methods developed for the analytical treatment of disordered systems, namely, the supersymmetry approach [5], cannot handle the effects of electron-electron interactions. Given this context, numerical approaches play a crucial role in the treatment of disordered, inter-

acting systems.

Several numerical approaches have been applied to the study of 2D disordered, strongly correlated systems [6–13]. Among the approximate approaches, Hartree-Fock calculations with residual interactions similar to the configuration interaction approaches of quantum chemistry have been applied to systems with spinless fermions and electrons with spin [6,8]. Exact diagonalization approaches have been useful but suffer from severe limitations in the accessible system size and number of particles [7,10,11,13]. From these studies, it has been observed that repulsive electron-electron interactions can have a delocalizing effect in small systems. In addition, it has been shown experimentally [1] that the spin degrees of freedom play a crucial role in the physics of these strongly interacting systems. The inclusion of the spin degrees of freedom renders the numerical calculations even more difficult and strongly reduces the number of fermions accessible (see e.g. [6,10–13]).

Quantum Monte Carlo (QMC) approaches provide a powerful alternative to the treatment of quantum many-body systems. These methods are in principle exact, apart from statistical errors and allow the treatment of much larger system sizes with many particles. The finite-temperature determinantal QMC approach has been applied to the two-dimensional disordered Hubbard model and signatures of a metal-insulator transition were obtained [14]. However, these calculations were carried out at finite temperature and could not access the ground state of the system. In previous work, we studied the ground state properties of the disordered 2D Hubbard model by the projector quantum Monte Carlo (PQMC) method [15]. We studied the properties of the Green's function, charge density and inverse participation ratio against model parameters and system size. While we observed some local charge reorganization, we could not detect any significant delocalizing influence of the Hubbard repulsion  $U$  on the many-body ground state. However, it

should be noted that all the physical quantities studied in Ref. [15] were obtained by integrating over all particles and effectively, the entire energy spectrum. Here we introduce a new approach which allows us to study the properties of a single added particle and therefore emphasizes the physical effects of interactions in the proximity of the Fermi edge.

This approach uses the inverse participation ratio (IPR) extracted from the charge density differences of two many-body ground states, as described below. The IPR,  $\xi$ , for a normalized single-particle wavefunction  $\psi(i)$  is given by  $\xi = [\sum_i |\psi(i)|^4]^{-1}$ , where  $i$  is the site index of the system. Clearly,  $|\psi(i)|^2$  can be identified as the one-particle charge density at the site  $i$ . This definition is usually carried over to many-body systems by renormalizing the total charge density at site  $i$ ,  $\rho(i, N_p)$ , which is obtained in the standard way from the ground state many-body wavefunction for  $N_p$  particles. The IPR  $\xi$  is then calculated with the effective charge density  $\rho(i, N_p)/N_p$ . We found that the IPR obtained from such a definition showed slight variations with model parameters and practically no variation with system size [15]. We believe that the physical reason for this weak variance is the fact that this procedure effectively integrates over all energies and therefore the dominant contribution comes from the states deeply below the Fermi energy, which remain strongly localized even in the presence of interactions. Therefore, it is necessary to find a method which is more sensitive to the contribution of states in the vicinity of the Fermi energy. Recently, we studied the localization properties of the disordered, *attractive* Hubbard model in two- and three-dimensions [16]. In Ref. [16], we showed that an IPR calculated for an added pair of particles is a very sensitive and relevant quantity to study the localization properties of the wavefunction. Based on our results for the attractive Hubbard model, we have introduced a related quantity in the repulsive case, the IPR for a single added particle, which turns out to be much more sensitive to the effects of interaction. This quantity has certain similarities to the single-particle tunneling amplitude. The latter has recently been studied by exact diagonalization methods for small clusters with spin-1/2 fermions [13]. This work provided indications for a delocalizing effect induced by repulsive interactions in disordered systems. However, the number of particles studied was rather restricted due to the limitations of the exact diagonalization methods. With our method and extensive, highly accurate PQMC simulations, we study considerably larger numbers of particles in presence of strong electron-electron interactions. In this study we report a significant delocalizing influence of the Hubbard repulsion on 2D disordered electronic systems. This paper is organized as follows : after this Introduction, we describe the method used and the tests performed in the next section. Our results and discussion are presented in detail in the third section.

## II. MODEL AND METHOD

The Hamiltonian studied in this paper is the disordered, repulsive Hubbard model given by:

$$H = H_A + H_I \\ = \left( -t \sum_{\langle ij \rangle, \sigma} c_{i, \sigma}^\dagger c_{j, \sigma} + \sum_{i, \sigma} \epsilon_i c_{i, \sigma}^\dagger c_{i, \sigma} \right) + U \sum_i n_{i \uparrow} n_{i \downarrow} \quad (1)$$

where  $c_{i\sigma}^\dagger$  ( $c_{i\sigma}$ ) creates (destroys) an electron at site  $i$  with spin  $\sigma$  and  $n_{i\sigma} = c_{i\sigma}^\dagger c_{i\sigma}$  is the corresponding occupation number operator. The hopping term  $t$  between nearest neighbor lattice sites characterizes the kinetic energy and the random site energies  $\epsilon_i$  are taken from a box distribution over  $[-W/2, W/2]$ . The parameter  $U$  measures the strength of the screened, repulsive Hubbard interaction ( $U > 0$ ). We have considered both the one- and two-dimensional cases, with periodic boundary conditions in all directions. In the 2D case, the sites  $i$  lie on a rectangular lattice of linear dimension  $N_x, N_y$ . The system size  $N = N_x \times N_y$  then follows accordingly in one- and two-dimensions. In the limit  $U = 0$ , this Hamiltonian reduces to the Anderson model (given by  $H_A$ ) which is a standard model for the study of disordered systems [17]. In the absence of disorder,  $W = 0$ , this Hamiltonian reduces to the usual Hubbard model, which is one of the best-studied models for correlated electronic systems [18].

We have studied this Hamiltonian by the projector quantum Monte Carlo (PQMC) method [19] and exact diagonalization calculations. The PQMC method was initially developed to study the ground state of the Hubbard model (clean limit of Eqn. (1)). The method can be generalized, in principle quite simply, to incorporate disorder via the random site energies. However, the actual implementation and convergence of the algorithm [15] is highly non-trivial compared to the pure case, as will be discussed in detail below.

The PQMC method consists in filtering out the true ground state  $|\psi_0\rangle$  of the many-body system from an appropriately chosen trial function  $|\phi\rangle$ :

$$|\psi_0\rangle = \lim_{\Theta \rightarrow \infty} \frac{e^{-\Theta H} |\phi\rangle}{\sqrt{\langle \phi | e^{-2\Theta H} | \phi \rangle}}. \quad (2)$$

This method is exact in principle, apart from statistical errors and the sign problem which appears for fermions at  $U > 0$ . The Hamiltonian plays the role of the projection operator through the term  $e^{-\Theta H}$ , where  $\Theta$  plays the role of the projection parameter. The trial wave-function is usually formed as a product of up and down spin states from the eigenstates of the non-interacting Hamiltonian. In our case, we chose the Fermi sea of  $H_A$  as the trial wave-function. In the PQMC procedure, the projection operator  $\exp(-\Theta H)$  is first Trotter decomposed as  $\left( \exp(-\Delta\tau H_A) \exp(-\Delta\tau H_I) \right)^L$  with  $\Theta = \Delta\tau \times L$ . This

introduces a systematic error of order  $(\Delta\tau)^2$  due to non-commutation of  $H_A$  and  $H_I$ . We have used the symmetric Trotter decomposition, which introduces a systematic error of  $(\Delta\tau)^3$ . The interaction is then decoupled by a discrete Hubbard-Stratonovich transformation, by the introduction of  $N \times L$  Ising-like fields. This Ising model with complicated effective interactions is then treated by a Monte Carlo (MC) procedure to obtain the ground state properties of the system. The quantity calculated during the simulation is the zero-temperature, equal-time Green's function,  $G_{ij} = \sum_{\sigma} \langle \psi_0 | c_{i,\sigma}^{\dagger} c_{j,\sigma} | \psi_0 \rangle$ . During the simulation this Green's function can be used to obtain all the other static correlation functions. In the algorithm used  $O(N^2)$  operations are required to update the Green's function after a MC step. This procedure introduces cumulative errors and therefore the Green's function has to be recalculated from scratch regularly during the simulation (every  $L_C$  steps), which requires  $O(N^3)$  operations. When the projection parameter  $\Theta$  becomes large, which is necessary for good convergence, the different components of the wavefunction tend to become parallel during the projection process. Therefore, it is necessary to reorthogonalise the components of the wavefunction regularly, every  $L_R$  time steps. In addition, it is well known that quantum simulations of fermionic systems suffer from the sign problem except in some special cases. However, it has been observed that disorder in fact diminishes the magnitude of the sign problem. In our simulations, the sign problem is well under control, with the number of negative signs being less than 1% of the total number of steps considered.

We have studied systems with particle number ( $N_p$ ) up to 25 fermions on lattice sizes of up to  $6 \times 8$  sites, with particle density always around quarter-filling. The simulations were carried out in the  $S_z = 0$  sector for even numbers of particles and the  $S_z = 1/2$  sector for odd number of particles. The specific quantity studied in this paper is the difference of charge densities  $\delta\rho(i)$  between systems with  $N_p$  and  $N_p + 1$  particles (see the next section for more details). Here, we discuss the convergence of the PQMC calculations. The charge densities involved in the calculation  $\delta\rho(i)$  are obtained from two independent simulations of the same disorder realization with different particle numbers,  $N_p$  and  $N_p + 1$ . Therefore, it becomes necessary to measure very accurately the distribution of this added particle over the lattice. Clearly, it is harder to measure  $\delta\rho(i)$  accurately than measuring the total charge densities  $\rho(i, N_p)$  in the ground state with  $N_p$  particles. We carried out extensive tests to verify the quality of our  $\delta\rho(i)$  data, by varying the PQMC parameters until convergence was obtained. We have tested for convergence by varying the following PQMC parameters: the projection parameter  $\Theta$ , the Trotter time-step  $\Delta\tau$ , the Monte Carlo parameters, the reorthogonalization interval  $L_R$  and the interval to recalculate the Green's function  $L_C$ . We have gone up to  $\Theta = 15$  and  $\Delta\tau = 0.05$ . For the physical parameters used in this paper, we find that

$\Theta = 10$  with  $\Delta\tau = 0.1$  are sufficient. This corresponds to a systematic error of  $10^{-3}$ . After varying the parameters  $L_R$  and  $L_C$  we decided to recalculate the Green's function with reorthogonalization of the components, after every 5 time-steps ( $L_R = L_C = 5$ ). We have also checked the MC parameters and find that 3000 sweeps are adequate for convergence, with 1000 sweeps for equilibration.

The disorder average was carried out over  $N_R$  different disorder realizations with  $N_R = 16$  in the PQMC simulations and  $N_R = 100$  for most exact calculations. The site-energies are randomly chosen for  $N_R$  disorder realizations at  $W/t = 1$  and then scaled proportionally to  $W/t$  for stronger values of disorder.

While our main motivation is the study of the 2D case, there are many useful reasons to study 1D systems. The 1D case can be studied conveniently by exact diagonalization methods, while changing the system size. Thus, we can study the variation of various properties such as the inverse participation ratio (IPR)  $\xi$ , with system size, exactly. These calculations provide a strong independent check on the PQMC data at small sizes. Further, the localization effect is much stronger in 1D and  $\delta\rho$  is usually strongly peaked in 1D as compared to 2D. Therefore, if the algorithm is capable of reproducing a localized peak, this provides a strong check on the method, at the given range of physical parameters (examples provided in the next section).

### III. RESULTS AND DISCUSSION

In order to study the localization properties of the system, we use the charge density distribution for an added particle at the Fermi level, given by:  $\delta\rho(i) = \rho(i, N_p + 1) - \rho(i, N_p)$ , where  $\rho(i)$  is the ground state charge density at site  $i$ . The values of  $\rho(i, N_p)$ ,  $\rho(i, N_p + 1)$  are obtained from two independent PQMC simulations for the same disorder realization. At  $U = 0$ , this  $\delta\rho(i)$  is identically equal to the one-particle probability distribution (added particle) at the Fermi edge. In the interacting case, this charge density distribution ( $\delta\rho(i)$ ) is not generally equal to a probability distribution. For example, it is not necessarily positive definite. However, in all the cases studied we find that this quantity is always positive. Therefore,  $\delta\rho(i)$  can be considered to be similar to a one-particle probability distribution. Thus, we can associate an inverse participation ratio (IPR) for an added particle, for a given disorder realization as:  $\xi = (\sum_i \delta\rho(i)^2)^{-1}$ . The disorder averaged IPR is given by  $\langle \xi \rangle$ . At  $U = 0$ , the IPR is a standard tool used to obtain the number of sites over which the particle is localized [5]. We have successfully used this approach in previous work on the disordered, attractive Hubbard model for a quantitative description of the localization properties of the ground state [16].

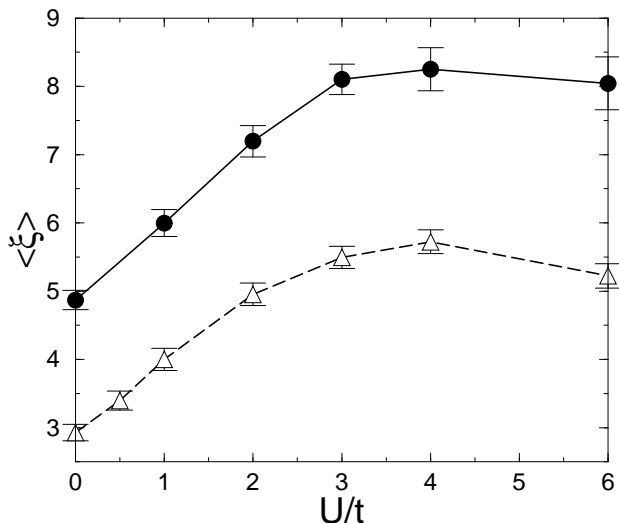


FIG. 1. IPR  $\langle \xi \rangle$  versus interaction strength  $U/t$ , at  $W/t = 7$ , for  $N_p = 6$  particles on a one-dimensional lattice with  $N = 12$  sites (triangles, average over 100 disorder realizations), and on a  $4 \times 3$  lattice (circles, average over 16 disorder realizations). Data comes from exact diagonalization. Here and in the following figures error bars denote statistical errors.

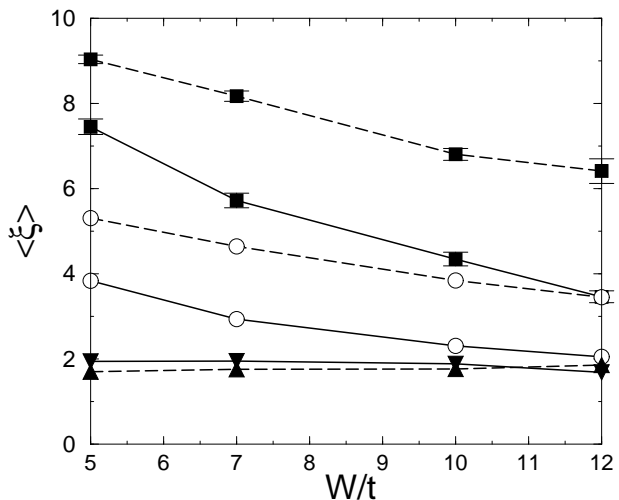


FIG. 2. IPR  $\langle \xi \rangle$  versus disorder strength  $W/t$ . Continuous curves are for the 1D system of 12 sites and  $N_p = 6$  particles, at  $U/t = 0$  (open circles) and  $U/t = 4$  (filled squares). Curves with dashed lines are for the  $4 \times 3$  lattice and  $N_p = 6$  particles, at  $U/t = 0$  (open circles) and  $U/t = 4$  (filled squares). Data come from exact diagonalization and are averaged over 100 disorder realizations (except the point for the  $4 \times 3$  lattice at  $U/t = 4$ ,  $W/t = 12$ , with  $N_R = 16$ ). The continuous curve with inverted triangles is the ratio  $\langle \xi(U/t) \rangle / \langle \xi(U/t = 0) \rangle$ , at  $U/t = 4$  for 1D and the dashed curve with triangles the same ratio for 2D.

In Figs. 1-2, we study the behavior of the IPR as a function of  $U/t$  and  $W/t$  to try and establish the interesting range of physical parameters in this system. In

Fig. 1, we compare the IPR  $\langle \xi \rangle$  for a 1D ring of 12 sites and a  $4 \times 3$  lattice in 2D as a function of interaction strength  $U/t$ . From the figure we see that increasing  $U/t$  from 0 tends to increase the IPR up to intermediate strengths of the interaction. Thus, the optimal value appears to be around  $U/t = 4$  in both 1D and 2D. Indeed, for  $U/t > 4$ , the value of IPR starts to decrease. In Fig. 2, we see the variation of  $\langle \xi \rangle$  for small system sizes for  $5 \leq W/t \leq 12$ . Since the ratio  $\langle \xi(U/t = 4) \rangle / \langle \xi(U/t = 0) \rangle$  is practically constant, this justifies our choice of parameter range for  $W/t$ . Disorder strength  $W/t < 5$  would lead to states with localization length larger than the accessible system size even at  $U/t = 0$ . Convergence of the PQMC calculations becomes progressively more difficult for larger disorder strengths. Therefore, we studied the variation of the IPR for  $W/t = 5, 7$  in the 2D case.

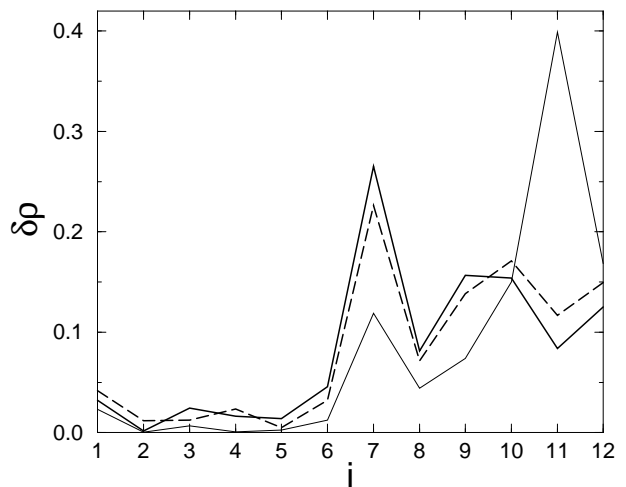


FIG. 3. Charge density difference  $\delta\rho(i)$  for a 1D lattice with  $N = 12$ ,  $N_p = 6$ ,  $W/t = 7$ ,  $U/t = 0$  (thin line, inverse participation ratio  $\xi = 4.31$ ), exact result for  $U/t = 2$  (thick solid line,  $\xi = 6.58$ ), and quantum Monte Carlo data for  $U/t = 2$  (dashed line,  $\xi = 6.93$ ).

Thus, it would seem ideal to study the IPR of 1D and 2D systems for  $5 \leq W/t \leq 7$  and  $U/t \approx 4$ . In 1D we could access these parameter values conveniently for the system sizes studied by exact calculations. However, this becomes much more difficult in 2D. This is because we study a small difference of large total charge densities in the PQMC simulations. We found that the accuracy of our method for  $\delta\rho(i)$  is good for values of the interaction  $U/t \leq 2$ . While we are not exactly at the optimal value of  $U/t$ , we are nevertheless in a region with sufficiently strong interactions. Indeed, it can be seen from Fig. 1 that  $U/t = 2$  already has a substantial delocalizing influence on the system. In Fig. 3, we present the PQMC calculation of  $\delta\rho(i)$  in 1D at  $U/t = 2$  as compared to exact calculations. We note that the  $\delta\rho(U = 0)$  is strongly peaked. Increasing  $U/t$  to 2 radically changes the picture and shifts the peak completely. The PQMC curve shown reproduces the quantitative picture of charge density dif-

ference. It should be noted that the calculation begins with a trial wavefunction corresponding to the  $U/t = 0$  data and changes completely to give the correct physical picture. Quantitatively, the usual errors seen at these values of the physical parameters were around 3 – 5%. The 2D case is more delocalized compared to 1D and we have observed that convergence is better in 2D. For example, we have  $\langle \xi \rangle = 7.19$  (exact) and 7.43 (QMC) for a  $4 \times 3$  lattice at  $U/t = 2$  and  $W/t = 7$ , averaged over 16 disorder realizations. This corresponds to an error of about 3% for the most extreme parameter values studied. However, for  $U/t = 4$ , the error increases to 8 – 10% and therefore we restrict our studies to  $U/t \leq 2$  in 2D.

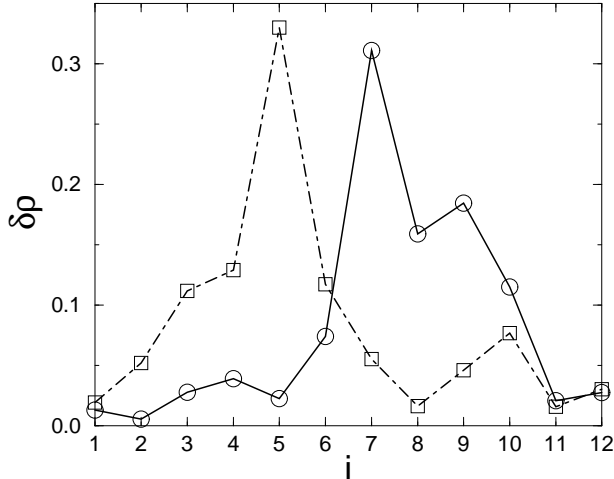


FIG. 4. Charge density difference  $\delta\rho$  for a 1D lattice with  $N = 12$ ,  $N_p = 6$ ,  $W/t = 7$ , and  $U/t = 4$ :  $\rho(N_p + 1) - \rho(N_p)$  (continuous curve with circles) and  $\rho(N_p + 2) - \rho(N_p + 1)$  (dot-dashed curve with squares). Data are from exact diagonalizations, for the same disorder realization as in Fig. 3. For comparison, see data for  $\delta\rho$  at  $U/t = 0$  in Fig. 3 (thin line).

Since we study a model of electrons with spin, it is interesting to consider even-odd effects in the particle number  $N_p$  and system size  $N$ . In Fig. 4, we consider the effect of progressively adding one and two particles to a 12 site ring with 6 electrons. From Fig. 3 and Fig. 4, we see that the first added electron at  $U/t = 2$  and 4, has an entirely different peak as compared to the non-interacting case. In Fig. 4, we see that the second added electron also occupies a different region, as seen from the position of the peak. This leads to the following physical image for the 1D case : each added electron finds its own location in space with optimal energy and it is well localized by external disorder and random distribution of charges of other electrons. This is in contrast with the non-interacting case, where the non-interacting orbital remains the same for odd and next even electron.

The situation is qualitatively different in 2D. Indeed, in Fig. 5, we show the charge density difference for one and two added particles on a  $6 \times 6$  lattice with 18 electrons. This quantity is obtained from PQMC simulations of the

system for a particular disorder realization, taken at  $W/t = 7$ . The data show that the initial  $U/t = 0$  configuration is very clearly localized for the given disorder realization and lattice size. It is seen from the figure that the introduction of a repulsive Hubbard interaction ( $U/t = 2$ ) leads to a substantial delocalization of the added particle. This is also borne out quantitatively, since the IPR increases practically by a factor of 3, as compared to  $U/t = 0$ . In the non-interacting case, both added particles occupy the same orbital. Therefore, the peak for the second added particle, is trivially identical to the first. It is remarkable that in the interacting case, the peak is transformed to a much more extended distribution over the lattice. Furthermore, the second added particle has practically the same distribution  $\delta\rho(i)$  as the first. Thus, there appears to be almost zero effective repulsion between the two added particles, despite the interaction strength  $U/t = 2$ . This is completely in contrast to the scenario in 1D with interactions, where we observe significant repulsion between the two added particles. We note that this is the case for every disorder realization studied.

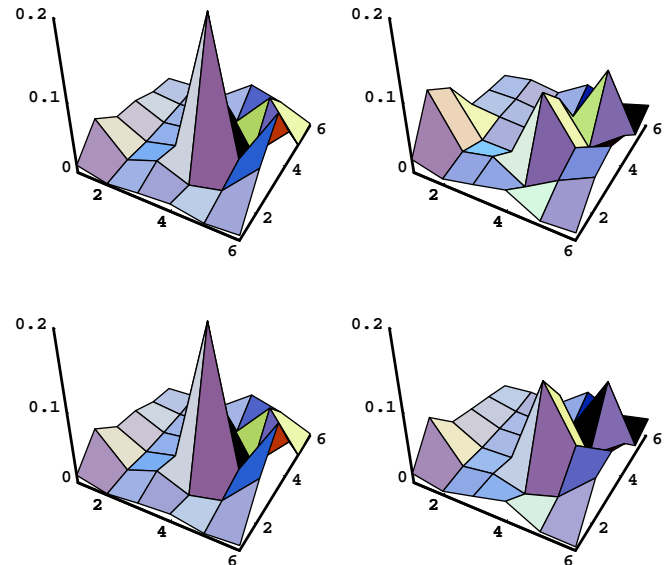


FIG. 5. Charge density difference  $\delta\rho$  for a  $6 \times 6$  lattice with  $N_p = 18$  particles,  $W/t = 7$ ,  $U/t = 0$  (left) and  $U/t = 2$  (right):  $\rho(N_p + 1) - \rho(N_p)$  (top) and  $\rho(N_p + 2) - \rho(N_p + 1)$  (bottom). Inverse participation ratios are  $\xi = 6.2$  (top left),  $\xi = 18.3$  (top right),  $\xi = 6.2$  (bottom left), and  $\xi = 16.7$  (bottom right).

We now turn to a more quantitative picture of the one and two dimensional systems. For this, it is necessary to average the data over different disorder realizations and to vary the system size. We start the analysis from the data for the 1D case. In Fig. 6, we present the IPR for interacting particles on 1D rings of 4–12 sites at

constant density of particles (quarter filling) and compare against the variation of the IPR at  $U/t = 0$ . We find a delocalization effect even for 1D rings. We note that the curve for  $U/t = 0$  is well saturated in 1D even at 8–12 sites. The  $U/t = 2$  curve shows signs of saturation. The delocalization effect is most visible for  $U/t = 4$ , as expected from Fig. 1, where unfortunately, we do not have access to PQMC data for comparisons. The ratio  $\langle \xi(U/t) \rangle / \langle \xi(U/t = 0) \rangle$  goes to 1.64 for  $U/t = 2$  and 1.94 for  $U/t = 4$ .

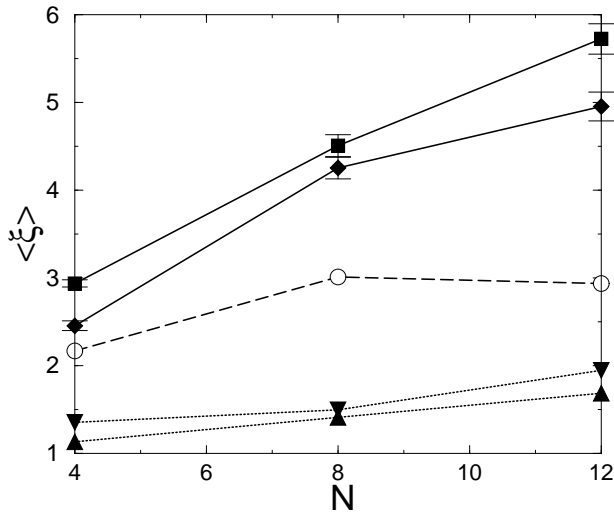


FIG. 6. Inverse participation ratio  $\langle \xi \rangle$  versus system size  $N$ , for 1D chains with periodic boundary conditions, at  $W/t = 7$ ,  $U/t = 0$  (circles),  $U/t = 2$  (diamonds), and  $U/t = 4$  (squares). Triangles and inverted triangles give the ratio  $\langle \xi(U/t) \rangle / \langle \xi(U/t = 0) \rangle$ , at  $U/t = 2$  and  $U/t = 4$ , respectively. Data come from exact diagonalization and are averaged over 100 disorder realizations.

In 2D previous exact diagonalization studies have gone up to 6 electrons on a  $4 \times 4$  lattice, or 4 electrons on a  $6 \times 6$  lattice [10,11,13]. Therefore, it is of great importance to access larger system sizes with more particles. In Fig. 7, we present the IPR for different lattice sizes in 2D, obtained from PQMC simulations. We have gone up to 48 sites ( $6 \times 8$  lattice) and 24-25 particles, which goes beyond any existing study of the ground state in the literature. We observe a delocalizing effect of the Hubbard repulsion manifested by an increase of the IPR with system size and interaction strength. There is a remarkable difference between the present result and the IPR for the full many-body ground state wavefunction obtained in Ref. [15]. In the previous work, we could notice no size effects over a large range of  $W$  and lattice sizes. In fact, the curves for different lattice sizes against  $U/t$  at a given value of  $W/t$  tended to collapse as seen in Figs. 8 and 9 of Ref. [15]. On the contrary, in the present work, we see from Fig. 7 that effects of lattice size on the IPR for an added particle are considerable. Furthermore, we see that the Hubbard repulsion has a

strong delocalizing influence, compared to the data for the non-interacting case. As explained in the previous sections, we attribute the difference between the present results and those presented in Ref. [15] to the fact that the IPR from  $\delta\rho$  measures directly the response in the vicinity of the Fermi level.

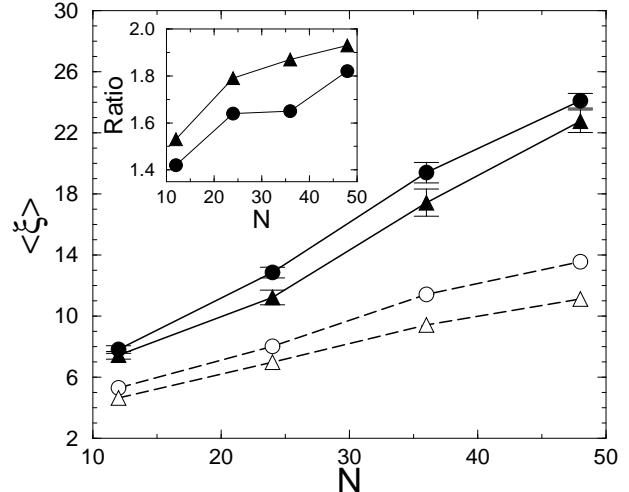


FIG. 7. Inverse participation ratio  $\langle \xi \rangle$  as a function of the number of sites  $N$ , for a 2D lattice, with quarter filling (i.e.,  $N_p = 6, 12, 18$ , and 24 fermions on  $4 \times 3, 6 \times 4, 6 \times 6$ , and  $8 \times 6$  lattices, respectively), with  $U/t = 0$  (empty symbols, average over  $10^3$  disorder realizations),  $U/t = 2$  (filled symbols, average over 16 disorder realizations), and  $W/t = 5$  (circles) and  $W/t = 7$  (triangles). The inset shows the ratio  $\langle \xi(U/t) \rangle / \langle \xi(U/t = 0) \rangle$ , at  $U/t = 2$ , for  $W/t = 5$  (circles) and  $W/t = 7$  (triangles). PQMC parameters:  $\Theta = 10$ ,  $\Delta\tau = 0.1$ , except for  $8 \times 6$  lattices where  $\Theta = 12$ ,  $\Delta\tau = 0.08$ .

The ratio  $\langle \xi(U/t) \rangle / \langle \xi(U/t = 0) \rangle$  can be considered as a quantitative measure of delocalization effect induced by repulsive interaction. From the inset of Fig. 7, it can be seen that this ratio rises with system size for a given density and we do not observe saturation at the system sizes studied. Our data for this ratio for small clusters in 2D are comparable to the enhancement ratio obtained in Ref. [13] though the quantity studied in Ref. [13] was slightly different i.e. the one-particle tunneling amplitude. From Figs. 6 and 7 we can compare the values of the ratio  $\langle \xi(U/t) \rangle / \langle \xi(U/t = 0) \rangle$  in 1D and 2D. At the system sizes studied these values are comparable for  $U/t = 2$ . However, it would be necessary to analyze the behavior of this ratio for larger system sizes in order to get a clear answer to whether the localization properties are indeed different in 1D and 2D. At the same time, we note that there seem to be qualitative differences based on even-odd effects for added particles in 1D and 2D (see Fig. 4 and Fig. 5 and discussion there). This difference favors the picture of stronger delocalization in 2D as compared to 1D.

Even if our data clearly show a repulsion induced delocalization effect, they do not permit us to draw a definite

answer about the existence of a metal-insulator transition for this system in the thermodynamic limit. Indeed, even though we have a significant number of fermions, we cannot go to larger system sizes because of the accuracy constraint of calculating charge differences. It should also be pointed out that our calculations done at  $U/t \leq 2$  are below the optimal value of the interaction strength. We expect that the delocalizing effect is even stronger at  $U/t = 4$ .

In conclusion, we have studied the ground state properties of the repulsive Hubbard model with disorder through the powerful QMC method. Highly accurate simulations permit us to obtain the difference of charge density between two ground states with  $N_p$  and  $N_p + 1$  fermions respectively. The analysis of this characteristic clearly shows that the Hubbard repulsion has a delocalizing effect in the system. We have observed some qualitative differences between 1D and 2D for this characteristic. However, the restrictions on system size and interaction strength do not permit us to draw a definite conclusion about the existence of a MIT in the thermodynamic limit in 2D.

We thank the IDRIS at Orsay for access to their supercomputers.

- 
- [1] E. Abrahams, S.V. Kravchenko, and M.P. Sarachik, Rev. Mod. Phys. **73**, 251 (2001).
- [2] P.A. Lee, and T.V. Ramakrishnan, Rev. Mod. Phys. **57**, 287 (1985).
- [3] B.L. Altshuler and A.G. Aronov, in *Electron-Electron Interactions in Disordered Systems*, edited by A.L. Efros and M. Pollak (North Holland, Amsterdam, 1985).
- [4] A.L. Efros and B.I. Shklovskii, J. Phys. C **8**, L49 (1975); M. Pollak, Phil. Mag. B **65**, 657 (1992); see also *Electron-Electron Interactions in Disordered Systems*, edited by A.L. Efros and M. Pollak, (North-Holland, Amsterdam, 1985).
- [5] K.B. Efetov, Supersymmetry in Disorder and Chaos (Cambridge University Press, 1997); A.D. Mirlin, Phys. Rep. **326**, 259 (2000).
- [6] T. Vojta, F. Epperlein, and M. Schreiber, Phys. Rev. Lett. **81**, 4212 (1998); T. Vojta, F. Epperlein, S. Kilina, and M. Schreiber, Phys. Status Solidi B **218**, 31 (2000).
- [7] X. Waintal, G. Benenti, and J.-L. Pichard, Phys. Rev. Lett. **83**, 1826 (1999).
- [8] G. Benenti, X. Waintal, J.-L. Pichard, and D.L. Shepelyansky, Eur. Phys. J B **17**, 515 (2000).
- [9] P.H. Song and D.L. Shepelyansky, Phys. Rev. **61**, 15546 (2000).
- [10] R. Kotlyar and S. Das Sarma, Phys. Rev. Lett. **86**, 2388 (2001).
- [11] F. Selva and J.L. Pichard, Europhys. Lett. **55**, 518 (2001).
- [12] G. Benenti, G. Caldara and D.L. Shepelyansky, Phys. Rev. Lett. **86**, 5333 (2001).
- [13] R. Berkovits and J.W. Kantelhardt, Phys. Rev. B **65**, 125308 (2002).
- [14] P.J.H. Denteneer, R.T. Scalettar, and N. Trivedi, Phys. Rev. Lett. **83**, 4610 (1999).
- [15] G. Caldara, B. Srinivasan, and D.L. Shepelyansky, Phys. Rev. B **62**, 10680 (2000).
- [16] B. Srinivasan and D.L. Shepelyansky, Eur. Phys. J. B **24**, 469 (2001); B. Srinivasan, G. Benenti, and D.L. Shepelyansky, Phys. Rev. B **66**, 172506 (2002).
- [17] A. MacKinnon and B. Kramer, Rep. Prog. Phys. **56**, 1469 (1993).
- [18] E. Dagotto, Rev. Mod. Phys. **66**, 763 (1994).
- [19] M. Imada and Y. Hatsugai, J. Phys. Soc. Jpn. **58**, 3752 (1989).